

New Segmentation Approach to Extract Human Mandible Bones Based on Actual Computed Tomography Data

Tamer M. Nassef

Computer Engineering Department, Misr University for Science & Technology, 6th of October, Egypt

Abstract In this paper, a new approach for segmenting different anatomical regions in dental Computed Tomography (CT) studies is presented. The approach consists of three steps: Hounsfield unit's threshold (HU) based on gray-level segmentation, multi-object with texture extraction and anatomical regions identification. First, a HU threshold window sets to separate between different regions upon their gray-level values; second, a set of objects are generated by and texture descriptors are calculated for selected windows from the image data sample. Finally, identification of different anatomical regions set for mandible bones cortical and cancellous. It is expected that the proposed approach will also help automate different semi-automatic segmentation techniques by providing initial boundary points for deformable models or seed points for split and merge segmentation algorithms. Preliminary results obtained for dental CT studies of human-mandible are presented.

Keywords CT Image Segmentation, Bone 3D Reconstruction, Multi-Objects Segmentation, Dental 3D Models

1. Introduction

Image scanners devices such as computed tomography (CT), magnetic resonance imaging (MRI) or positron emission tomography (PET) are nowadays a standard instrument for diagnosis. Among these devices, CT-scanners are today widely used at radiotherapy departments all over the world it has several advantages. The main advantages of a CT-scanner are to obtain physical information, like patient anatomy, size, shape, and in homogeneities; the other is to obtain the electron density from the different anatomical structures of the patient for the radiotherapy treatment planning[1]. Image segmentation is one of the primary steps in image analysis for object identification. The main aim is to recognize homogeneous regions within an image as distinct and belonging to different objects, where the segmentation process can be based on actual Digital Imaging and Communications in Medicine DICOM data to find the maximum homogeneity in grey levels within the regions identified.

A variety of techniques have been proposed for CT image segmentation methods. These methods can be classified into three categories. The first category includes analytic methods, in which segmentation algorithms are treated directly by considering some measure (e.g. Hounsfield Unite), which by a priori knowledge is assumed to be the

appropriate measure, Gabriella Tognola et al (2006) extract the mandible contour by histogram equalization and thresholding and proposed another method by gradient vector flow snake parameters were optimized in order to achieve more accurate contours segmentation of nerve mandibular scans[2]-[4]. Paola Campadelli et al (2009) apply hierarchical gray level based on framework to segment heart, bones, liver, kidneys, and spleen directly related to the Hounsfield units (HU) based on gray level techniques, learning techniques, model fitting techniques, probabilistic atlases, and level set anatomical knowledge to obtained three dimensional (3-D) binary image[5]. Typically this measure was incorporated into the original segmentation algorithm as well.

The second category includes supervised evaluation methods. In these methods, the results of a segmentation algorithm are compared to a "standard" reference image that is manually segmented beforehand, and the amount of discrepancy becomes the measure of segmentation effectiveness. Gaivile Pilecikiene et al (2007) choose dead person for the study the precision of CT examination increased – oluntary and involuntary movements of research object were excluded (like breathing or muscle tonus movements), this make the segmentation more easier since the high resolution images captured by increasing the dose to get more than 1500 slice from the CT scanner[6], Ming Chen et al (2007) choose the same condition with another method by comparing between dead and alive person. The author used commercial software to segment the DICOM images based on threshold and region growing methods to extract the mandible for a patient[7]. Zhan Liu et al (2007) used the

* Corresponding author:

tamer.nassef@k-space.org (Tamer M. Nassef)

Published online at <http://journal.sapub.org/ajbe>

Copyright © 2012 Scientific & Academic Publishing. All Rights Reserved

same commercial software in his studies, but here the Temporomandibular Joint (TMJ) appear clearly in the 3D model geometry information of the cortical bones, the cancellous bones and the teeth was exported from commercial software and this may accomplished by semi-automated method[8]. This is the most commonly used method for medical segmentation. However, manually generating a reference image is a difficult, subjective, and time-consuming job, and generally cannot guarantee that one manually-generated segmentation image is better than another. Consequently, comparison using such reference images cannot ensure accurate evaluations.

The third category includes unsupervised evaluation. In these methods, the segmentation results are evaluated by judging the quality of the segmented image directly to evaluate some pre-defined criteria, such as the partitioning of foreground objects from the background, J.M. Reina et al (2006) present a 3D surface model of mandible based on morphological analysis with standard distances without case study and this near to the information theory. Since the shape of each organ is not consistent throughout all slices of a 3D medical image and the gray level intensities overlap considerably for soft tissues, texture is especially important in medical image segmentation because of its homogeneity within the same tissue and across different slices. Once textures have been calculated and their scalar values assigned to pixels, the pixels can be clustered or classified (when the tissues' labels are available) for the purpose of segmentation[9]. These evaluation measures are typically used with gray-level images and are not designed for general-purpose applications. However, modeling of biological tissues, such as bone related organs, is a difficult task because of their inherent inhomogeneous and anisotropic character, although inhomogeneous character is in some sense "directly" accessible via imaging techniques. Unfortunately, this is not the case for the trajectories of anisotropic elasticity. Many investigators have evaluated 3-D models from Computed Tomography (CT) 2-D images. The results of these studies have been approximated for the conversion of images formats. Mechanical anisotropy means that the mechanical properties of the material are different when measured in different directions in the same sample. For reasons of simplification, modulus of elasticity of the mandibular bones, was given constant values and considered isotropic to facilitate simulation.[10]

The use of numerical methods such as finite element methods (FEM) has been adopted in solving complicated geometric problems, as it is very difficult to achieve an analytical solution. FEM is a technique for obtaining a solution to complex mechanical problems by dividing the domain problem into a collection of much smaller and simpler domains (elements) where field variables can be interpolated using shape functions[13]. In 1977, Weinstein[11] was the first to use FEM in implant dentistry. Subsequently, FEM was rapidly applied in many aspects of implant dentistry. Atmaram and Mohammed[12]-[14] analyzed the stress distribution in a single tooth implant, to

understand the effect of elastic parameters and geometry of the implant, implant length variation, and pseudo-periodontal ligament incorporation. Borchers and Reichart[14] performed a three-dimensional (3-D) FEM of an implant at different stages of bone interface development. Cook, et al.[16] applied it in porous rooted dental implants. Meroueh, et al.[17] used it for an osseointegrated cylindrical implant. Williams, et al.[18] carried it out on cantilevered prostheses on dental implants. Akpinar, et al.[19] simulated the combination of a natural tooth with an implant using FEM.

In the present study, a new approach for segmentation based on actual CT data are used to extract an accurate human mandible with TMJ and teeth to help for generating robust 3D surfaces and volumetric models. The proposed technique used the statistical texture method applying entropy transformation combined with information captured from HU based on gray-level techniques, finally a level sets and geometric contour used to build the prototype geometry for the full-human mandible.

2. Material and Methods

Dentate and edentulous patient's mandible was scanned with SIEMENS/Esprit CT machine 120 KeV energy. The pixel size of the scanner is 512x512 pixels, and 0.4 mm is equal to the distance between CT slice planes. Totally 400 images were obtained, raw data was in DICOM format.

A HU and Gray-level phase

The electron density is obtained from the CT-scanner via the so-called Hounsfield units (HU). These are defined as:

$$HU = 1000 \left(\frac{\mu - \mu_{water}}{\mu_{water}} \right) \quad (1)$$

where (μ) referred to the linear attenuation coefficient for the respective material compared with water. The linear attenuation coefficient depends on parameters such as electron density, atomic number and the beam quality of the CT-scanner. In the implementation of the Hounsfield scale in this study the Hounsfield scale stretches between $HU = -1024$ and $HU = 3071$. A HU of -992 represents air outside the patient and a HU of larger than 2832 represents iron.

DICOM format files carrying all information about CT scanned, different tissues segmented based on HU range by verified windows defining the tissues pixel positions, each slice has different HU range and this helps in applying the threshold technique to evaluate the difference in bone density for different bone types, where any noise maybe produced by the reflection rays on filling materials affects the HU range and the 3-D reconstruction of the mandible can be reduced by used segmentation techniques based on selecting the HU values, H_{min} and H_{max} .

Figure 1 shows CT slices and its histogram depends on HU range created by MATLAB program, this helps to extract bones from slices according to its HU range. HU_{min} and HU_{max} are reported at table 1, and the different tissues have different values of HU

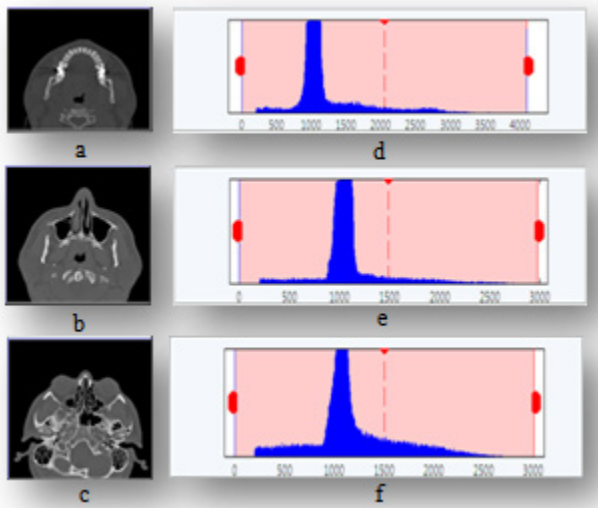


Figure 1. Histogram of CT slices samples by HU range; displayed beside each slice

Table 1. HU range for the slices samples

Slice Number	HU _{min}	HU _{max}	HU _{avg}
a	0	4000	2000
b	0	2947	1486
c	0	3004	1502

To get the parallel gray-level (GL) values from HU values equation (2) are used.

$$GL = \frac{n * m}{HU_{Range}} \quad (2)$$

where $n * m$ are refer to the pixel size of the CT-scanner.

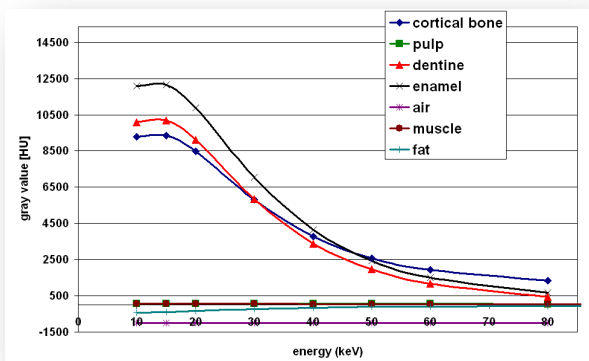


Figure 2. Hounsfield units in GL for different anatomical structures versus energy KeV

The calculations at Fig. 2 are performed based on ICRU 44, Herkströter *et al* (1990) and Hubell and Seltzer (1996), and created by MATLAB program.

A Multi-object reconstruction and texture phase

The multi-object reconstruction helps to extract the mandible bone from skull; that the model will have specific information about mandible, proposed segmentation technique is used to extract it from the CT slices based on region growing technique, which is implemented with MATLAB program. Triangulation process method is used to

generate the 2½-D models and the marching cubes for the final 3-D model; this is applied for all slices.

After the multi-object reconstruction process; the objects must be enveloped by texture material as shows in Fig. 3.

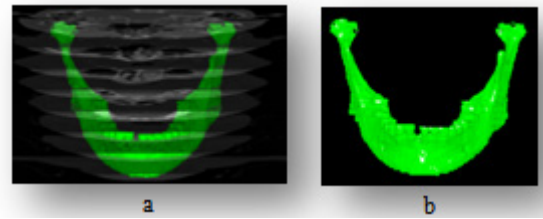


Figure 3. The texture material, (a) CT planes with mandible, (b) mandible textured with bone material

B Anatomical regions identification phase

At this phase a computer program was written in MATLAB code for implementing the segmentation process applied on all DICOM planes, all planes are assembled. Multi-objects regions enveloped with texture material to verify their prosperities, by evaluating the vertex (x,y,z) of model from origin (0,0,0) pixels positions can be calculated. Intensity can be measured by calculating the pixels values multiplied by pixels numbers (3). Preliminary intensity measurements are shows in table 2.

$$Intensity(x) = \sum_{i=1}^N (P_n * P_v) \quad (3)$$

where P_n equal to pixel position and P_v equal to pixel value and i refer to pixel number.

Table 2. Intensity measurements of teeth

Plane Number	Number of Pixels	Center (X,Y,Z)	Total Intensity	Mean Intensity
13	31	298.14,218.23,13.0	81045	2614.4
14	118	275.32,214.21,14.0	320484	2715.96
15	298	274.24,211.10,15.0	815393	2736.2
16	582	274.29,207.78,16.0	1594598	2739.9
41	1036	271.41,271.51,41.0	2734922	2639.9
42	606	263.28,270.21,42.0	1631745	2692.6
43	272	241.72,268.87,43.0	734706	2701.1
All	72113	266.33,230.95,29.67	218144702	3025.0

Table 3. Validation of output models

Category	Phantom Software	DICOM	Multi-object Model
Artifacts noise	√	√	null
Soft tissue interference	12%to 20%	null	2%
TMJ	null	√	√

3. Results

There are three different models provided from this approach, Fig.4 represents models for the dentate patient, who used to validate the technique by comparing it with the provided model from the phantom software at the CT scanner, full skull with and without skin with different colors to show the different objects. Table 3 shows the comparison

between Multi-object models with DICOM images and phantom software at the CT scanner, where the TMJ that hides behind the skull bone appears with Multi-object models, the artifacts noise from felling metals or implants and undesired soft tissues will be reduced.

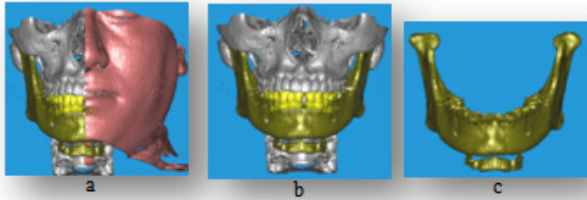


Figure 4. Multi-objects 3-D model, (a) all objects with skin section, (b) full skull without skin, (c) full mandible with Hyoid bone and TMJ

For edentulous patients Fig.5 represents models for two types of bone, where the trabicular pattern is evaluated for the cancellous bone, and Fig.6 shows the difference measurement between edentulous mandible before and after implant surgery, where the 3-D model shows the amount of healing bone after 6 months and the exactly amount are measured at second phase of the modeling technique as shown at the fig., all figures with 512x512 resolutions.

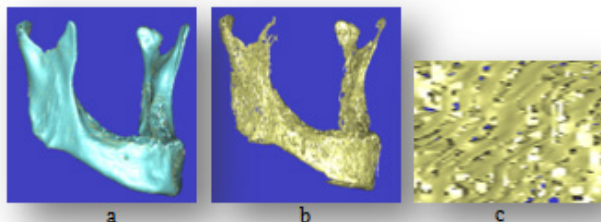


Figure 5. Mandible bones, (a) Cortical bone, (b) Cancellous bone, (c) Trabicular pattern for cancellous bone (zooming by 30X)

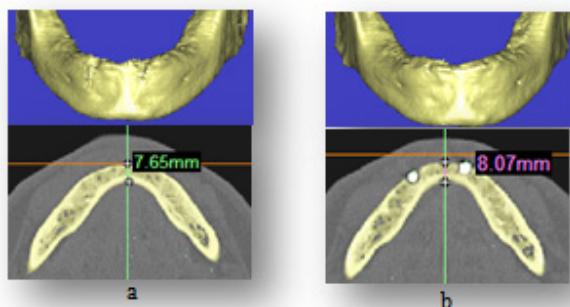


Figure 6. measures of healing bone around implants, (a) the mandible without implants, (b) the mandible with implants after 6 months

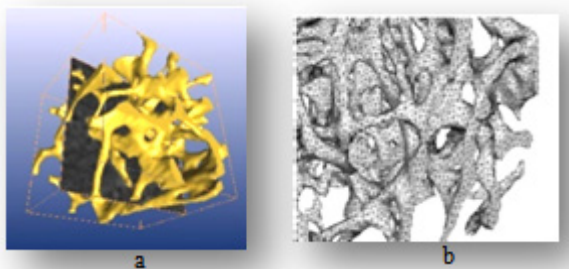


Figure 7. Trabicular pattern for cancellous bone, (a) finally textured trabicular model, (b) finite element model meshed by tetrahedral elements

Finally the cancellous bone pattern can be exported to any

finite element program with STL format as shown in Fig. 7, where Abacus program are used to provide a finite element model for the trabicular pattern divided by tetrahedral elements.

4. Conclusions and Future Works

Many investigators have evaluated 3-D models from CT 2-D images. The results of these studies have been approximated for the conversion of images formats, this study provide a realistic 3-D model from 2-D segmented images scanned with CT scanner device based on actual CT data carried by DICOM files formats. Preliminary results are reported; pixels intensity values and pixels numbers are significant to verify the volumetric 3-D model of objects, this model can helps in dental diagnosing and to evaluate the orthogonal mechanical properties values especially for edentulous patients. The noises produced for filling cavity materials or dental implants are eliminated by combined classical segmentation techniques. Tetrahedral elements are suitable to divide the mandible model to finite elements for mechanical analysis studies like implant stress-strain; multi-objects technique separate mandible to objects for decreasing the number of nodes and elements to reduce the number of FEA equations; this will accelerate the idealization process at FEM models.

REFERENCES

- [1] Shum, H.Y., Chan, S.C. and S.B. Kang, Image-Based Rendering, Springer Science-Business Media, LLC, Spring Street, New York, USA, 2007.
- [2] Tognola, G., Parazzini, M., Pedretti, G., Ravazzani, P., Grandori, F., Pesatori, A., Norgia, M., and C. Svelto, "Optimization of 2-D to-3-D Reconstruction Technique for Maxillofacial Surgery Applications", Proceedings of IST - International Workshop on Imaging Systems and Techniques, pp.186-189, IEEE, Italy, April 2006.
- [3] Tognola, G., Parazzini, M., Pedretti, G., Ravazzani, P., and C. Svelto, "Three-dimensional reconstruction and image processing in mandibular distraction planning," IEEE transaction on instrumentation and measurement, Volume. 55, (6), pp.1959-1964, December 2006.
- [4] Tognola, G., Parazzini, M., Pedretti, G., Ravazzani, P., Grandori, F., Pesatori, A., Norgia, M., and C. Svelto, "Novel 3D reconstruction method for mandibular distraction planning," Proceedings of IST - International Workshop on Imaging Systems and Techniques, pp.82-85, IEEE, Italy, April 2006.
- [5] Campadelli, P., Casiraghi, E., Pratisoli, S., and G. Lombardi, " Automatic abdominal organ segmentation from CT images," Electronic Letters on Computer Vision and Image Analysis, Volume 8(1), pp.1-14, January 2009.
- [6] Pileickiene, G., Varpiotas, E., Surna, R., and A. Surna, " A

- three-dimensional model of the human masticatory system, including the mandible, the dentition and the temporomandibular joints," *Stomatologija, Baltic Dental and Maxillofacial Journal*, Volume. 9 (1), pp.27-32, 2007.
- [7] M. Chen, L. Ni, Yu Zhang, Yuan Zhang "Comparison study on the 3D reconstruction of mandible according to Virtual Chinese Human slice data and CT data," *World Journal of Modelling and Simulation*, Volume. 3 (3), pp. 235-240, May 2007.
- [8] Liu, Z., Fan, Y., and Y. Qian, "Biomechanical simulation of the interaction in the Temporo-mandibular Joint within dentate mandible: A Finite Element Analysis," *Proceedings of ICME - International Conference on Complex Medical Engineering*, pp.1842-1846, IEEE, China, 2007.
- [9] Reina, J.M., García-Aznar, J.M., Domínguez, J., and M. Doblaré, "Numerical estimation of bone density and elastic constants distribution in a human mandible," *J. Biomech. Eng.*, (doi: 10.1016), Elsevier (0021-9290), March 2006.
- [10] Nassef, T. M., Alkhodary, M., Marei, M. K., Awadalla, and, M. A., and Moustafa, R., "A New Interactive 3-D Numerical Model of the Human Mandible for Peri-Implant Analysis in-Vivo Compared With Cone Beam Computed Tomography 3-D Quality," *American Journal of Biomedical Engineering* 2012; 2(1): 9-16
- [11] Weinstein, A.M, Klawitter, J.J, Anand, S.C, and R. Schuessler, "Stress Analysis of Porous Rooted Dental Implants," *Proceedings of Implantologist, Conf*, Volume 1, pp. 104-109, 1977.
- [12] Atmaram, G.H, and H. Mohammed," Stress analysis of single-tooth implants. I. Effect of elastic parameters and geometry of implant" *Proceedings of Implantologist, Conf*, Volume 3, pp. 24-29, 1984.
- [13] Atmaram G.H, and H. Mohammed, "Stress analysis of single-tooth implants II. Effect of implant root-length variation and pseudo periodontal ligament incorporation," *Proceedings of Implantologist, Conf*, Volume 3, pp.58-62, 1984.
- [14] Mohammed, H., Atmaram, G.H., and F.J. Schoen, "Dental implant design: a critical review," *J Oral Implantol*, Volume 8, pp. 393-410, 1979.
- [15] Borchers.L, and P. Reichart," Three-dimensional stress distribution around a dental implant at different stages of interface development,"*J Dent Res*, Volume 62, pp. 155-159, 1983.
- [16] Cook, S.D., Weinstein, A.M., J.J. Klawitter," A three-dimensional finite element analysis of a porous rooted Co-Cr-Mo alloy dental implant " *J Dent Res*, Volume 61, pp. 25-129, 1982.
- [17] Meroueh, K.A., Watanabe, F., and P.J. Mentag, "Finite element analysis of partially edentulous mandible rehabilitated with an osseointegrated cylindrical implant," *J Oral Implantol*, Volume 13, pp. 215-238, 1987.
- [18] Williams, K.R., Watson, C.J., Murphy, W.M., Scott, J., Gregory, M., and D. Sinobad," Finite element analysis of fixed prostheses attached to osseointegrated implants " *Proceedings of Quintessence Int, Conf*, Volume 21, pp. 563-570, 1990.
- [19] Akpınar, I., Demirel, F., Parnas, L., and S. Sahin," A comparison of stress and strain distribution characteristics of two different rigid implant designs for distal extension fixed prostheses," *Proceedings of Quintessence Int, Conf*, Volume 27, pp. 11-17, 1996.